



PEEK composites reinforced by nano-sized SiO₂ and Al₂O₃ particulates

M.C. Kuo^{a,b}, C.M. Tsai^a, J.C. Huang^{a,*}, M. Chen^a

^a Institute of Materials Science and Engineering, Center for Nanoscience and Nanotechnology, National Sun Yat-Sen University, Kaohsiung, Taiwan 804, ROC

^b Department of Applied Fiber Style, Kun Shan University of Technology, Tainan, Taiwan 700, ROC

Received 20 May 2004; received in revised form 29 September 2004; accepted 11 October 2004

Abstract

The poly(ether-ether-ketone) (PEEK) polymer filled with nano-sized silica or alumina measuring 15–30 nm to 2.5–10 wt.% are fabricated by vacuum hot press molding at 400 °C. The resulting nanocomposites with 5–7.5 wt.% SiO₂ or Al₂O₃ nanoparticles exhibit the optimum improvement of hardness, elastic modulus, and tensile strength by 20–50%, with the sacrifice of tensile ductility. With no surface modification for the inorganic nanoparticles, the spatial distribution of the nanoparticles appears to be reasonably uniform. There seems no apparent chemical reaction or new phase formation between the nanoparticle and matrix interface. The crystallinity degree and thermal stability of the PEEK resin with the addition of nanoparticles are examined by X-ray diffraction, differential scanning calorimetry, and thermogravimetry analyzer, and it is found that a higher crystallinity fraction and degradation temperature would result in the composites as compared with the unfilled PEEK.

© 2004 Elsevier B.V. All rights reserved.

Keywords: Nanocomposites; PEEK; Mechanical properties; Thermal stability

1. Introduction

The inclusion of inorganic fillers into polymers for commercial applications is primarily aimed at the cost reduction and stiffness improvement [1,2]. It is worth noting that the inclusion of micrometer sized particulates into polymers, a high filler content (typically greater than 20 vol.%) is generally required to bring the above stated positive effects into play. This would detrimentally affect some important properties of the matrix polymers such as processability, appearance, density and aging performance. Therefore, composites with improved performance and low particle contents are highly desired. With this concern, the newly developed nanocomposites, i.e., polymers or metals reinforced by nano scaled fillers, would come into the competitive candidates.

The high performance poly(ether-ether-ketone) (PEEK) polymer was first prepared by Bonner in 1962 [3]. It is a derivative of poly(aryl-ether-ketones). PEEK is chemically

recognized as a linear poly(aryl-ether-ketone) and is a melt processable aromatic polymer; the melting point T_m lies between 330 and 385 °C, depending on the relative proportion of ether-ketone groups linking the phenylene rings [4]. The degree of crystallinity depends on the thermal histories and the processing conditions, such as cooling rates and annealing treatments.

It is well known that the continuous carbon fiber (CF) reinforced PEEK polymer composites possess extraordinary specific strength and stiffness along the longitudinal (or fiber) direction with fiber content up to 61 % by volume (vol). It has been proposed that the processing temperature for the PEEK based composites needs to be as high as 400 °C [5,6]. On the other hand, short carbon fiber reinforced PEEK composites possess reasonably high tensile modulus and strength with 30 vol.% fiber, and are also characterized by their high fracture toughness [7,8].

Polymer nanocomposites have attracted considerable attention and interest worldwide during the last decade. Among the fabrication methods for polymer nanocomposites, the sol-gel method appears to be the most promising one. The nanoparticles were first dispersed, and then mixed with the

* Corresponding author. Tel.: +886 7 5252000x4063; fax: +886 7 5254099.

E-mail address: jacobc@mail.nsysu.edu.tw (J.C. Huang).

polymer gel at the molecular or near molecular level. It is well known that PEEK is of good resistance to most organic solvents except concentrated sulfuric acid (95–98%) and methyl sulfonic acid ($\text{CH}_3\text{SO}_3\text{H}$) [4,9]. Accordingly, it is highly unlikely or impossible to fabricate commercially the nanoparticle-filled PEEK composites by means of the sol–gel method. However, PEEK polymers reinforced with nanoparticles processed via solid (or partial melting) state routes have been reported [10–12]. The PEEK fine powders, $\sim 100\ \mu\text{m}$, were fully mixed with the Si_3N_4 nanoparticles, small than 100 nm, and subsequently formed by compression molding [10]. As a result, the incorporation of Si_3N_4 nanoparticles into PEEK caused a significant improvement in the tribological characteristics, resulting considerably in decreased frictional coefficient and wear rate. In addition, PEEK based composites reinforced with other nanoparticles such as ZnO_2 [10] and SiC [12] have also been studied, and similar results were reported.

Moreover, PEEK nanocomposites containing vapor grown carbon nanofibers (CNF), with a mean diameter $\sim 155\ \text{nm}$ and an aspect ratio ~ 1000 , have been fabricated [13] by means of twin screw extrusion. The CNF filled PEEK nanocomposites revealed a linear increase in tensile stiffness and strength with increasing CNF content up to 15 wt.%, while the tensile ductility was maintained up to 10 wt.% CNF.

The inclusion of much cheaper (in comparison with CNF or carbon nanotubes CNT) nano SiO_2 or Al_2O_3 particles (with diameters $\sim 15\text{--}30\ \text{nm}$) into PEEK is of basic interest for the purposes of processability and mechanical enhancement. The present study is focused on the simple compression molding to fabricate the PEEK nanocomposites containing 0–10 wt.% nanometer sized silica or alumina particles without any surface modification. The mechanical property improvement and the interaction between the filled particles and the PEEK matrix are under examination. Moreover, the effects of the nanoparticle inclusion on the nonthermal crystallization of PEEK chain segments and enhancement of thermal stability of PEEK composite are also under investigation.

2. Experimental procedures

The PEEK powders (grade Victrex 450P, diameter $\sim 2\text{--}3\ \text{mm}$) was purchased from the ICI Company, USA, and was further grinded into fine powders measuring $50\ \mu\text{m}$. The density of PEEK polymer is $1.30\ \text{Mg m}^{-3}$. The SiO_2 and Al_2O_3 nanoparticles with diameter ~ 30 or $15\ \text{nm}$ and purity $\sim 99.9\%$ were purchased from the Plasmachem GmbH Company, Germany/Russia. The SiO_2 particles are irregular in shape with an aspect ratio near 1, and the Al_2O_3 powders are basically spherical. The density is $2.65\ \text{Mg m}^{-3}$ for SiO_2 and $3.98\ \text{Mg m}^{-3}$ for Al_2O_3 .

Since it is not possible to measure the volume amount for the nanoparticles when they are in powder forms, the addition of nanoparticles was measured by weight percent (wt.%), from 2.5 to 10 wt.%. Owing to the higher densities of SiO_2

Table 1

Comparison of the weight and volume percentage (wt.% and vol.%) of the nano SiO_2 and Al_2O_3 particles added in the PEEK composites

SiO_2				
wt.%	2.5	5.0	7.5	10.0
vol.%	1.2	2.5	3.7	4.9
Al_2O_3				
wt.%	2.5	5.0	7.5	10.0
vol.%	0.8	1.6	2.5	3.3

The densities for PEEK, SiO_2 , and Al_2O_3 are 1.30 , 2.65 , and $3.98\ \text{Mg m}^{-3}$, respectively.

and Al_2O_3 , the transformed volume percent (vol.%) would be lower, as summarized in Table 1. Note that the Al_2O_3 particles are added in lower amounts in volume as compared with the SiO_2 counterparts. Meanwhile, the maximum amount in volume fraction was 4.9 vol.% for SiO_2 and 3.3 vol.% for Al_2O_3 , considerably lower than the 15–50 vol.% for the conventional polymeric or metallic composites. This means that the current nanocomposites would not alter much the processability or density of the PEEK matrix.

PEEK nanocomposites were fabricated by means of compression molding at $400\ ^\circ\text{C}$ under a load of 60 MPa. Prior to compression molding, the fine PEEK powders were completely mixed with the nanoparticles (SiO_2 or Al_2O_3) through ultrasonic vibration in alcohol medium, and then the well dispersed sol was dried at $80\ ^\circ\text{C}$ to remove the excess alcohol.

Room temperature tensile testing was conducted in accordance with the ASTM standard E8M-89. The gauge length was set to be 40 mm, and the crosshead speed was $1\ \text{mm min}^{-1}$, corresponding to a strain rate of $4 \times 10^{-4}\ \text{s}^{-1}$. Strain gauge was attached to the gauge for measurements of elastic modulus and failure elongation.

A Shimadzu HMV-2000 Vickers microhardness tester was applied to evaluate the microhardness enhancement. The specimens were subjected to a load of 50 g for time duration of 15 s. The JEOL-JSM 6400 scanning electron microscope (SEM) equipped with energy dispersive spectrometry (EDS), as well as the JEOL 3010 transmission electron microscope (TEM), were used to evaluate the nanoparticle dispersion condition. The thin foil TEM specimens were prepared by

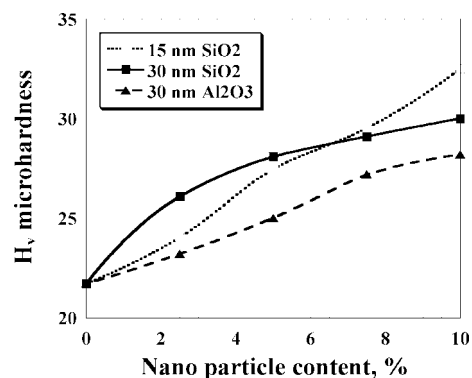


Fig. 1. Variations of the microhardness of the nanocomposites as a function of the nanoparticle content in wt.%.

Table 2
Comparison of the theoretically predicted (Theo) and experimentally measured (Exp) mechanical data

Filler	Variable	0 wt.%		2.5 wt.%		5 wt.%		7.5 wt.%		10 wt.%	
		Theo	Exp	Theo	Exp	Theo	Exp	Theo	Exp	Theo	Exp
15 nm SiO ₂	H_v	–	21.7	22.6	24.0 (11%)	23.7	27.5 (27%)	24.6	29.5 (36%)	25.5	32.5 (50%)
	E_c , GPa	–	3.9	3.9	4.1 (5%)	4.0	4.1 (5%)	4.0	4.3 (10%)	4.1	4.5 (15%)
	UTS, MPa	–	89	90	96 (8%)	91	100 (12%)	91	102 (15%)	92	101 (14%)
30 nm SiO ₂	H_v	–	21.7	22.6	26.1 (20%)	23.7	28.1 (29%)	24.6	29.1 (34%)	25.5	30.0 (38%)
	E_c , GPa	–	3.9	3.9	4.2 (8%)	4.0	4.5 (15%)	4.0	4.9 (26%)	4.1	5.3 (36%)
	UTS, MPa	–	89	90	94 (6%)	91	105 (18%)	91	91 (2%)	92	89 (0%)
30 nm Al ₂ O ₃	H_v	–	21.7	22.7	23.2 (7%)	23.0	25.0 (15%)	23.7	27.2 (25%)	25.9	28.2 (30%)
	E_c , GPa	–	3.9	4.2	4.1 (5%)	4.5	4.4 (13%)	4.8	4.6 (18%)	5.0	5.1 (31%)
	UTS, MPa	–	89	90	97 (9%)	91	105 (18%)	92	108 (21%)	93	94 (6%)

The increment percentage of the experimental data with respect to the unfilled PEEK is also included in parentheses.

microtome with a diamond knife, and examined in TEM operated at 150–200 KeV. Also, a Siemen D5000X X-ray diffractometer with Cu K α radiation was applied to investigate the effects of the filled nanoparticles on the crystallization degree of the PEEK resin.

The effects of the filled nanoparticles on the thermal behavior of the PEEK resin were evaluated using a Perkin-Elmer differential scanning calorimeter (DSC-7). The weights of all samples were about 6 mg, and these samples were heated to 410 °C at a heating rate of 10 °C min⁻¹ under nitrogen atmosphere, and held for 5 min to remove the previous thermal history. Non-isothermal crystallization was investigated by cooling the samples from 410 to 50 °C at various cooling rates of 5, 10, 15, 20, 25, and 30 °C min⁻¹. The effect of the filled nanoparticles on thermal stability of

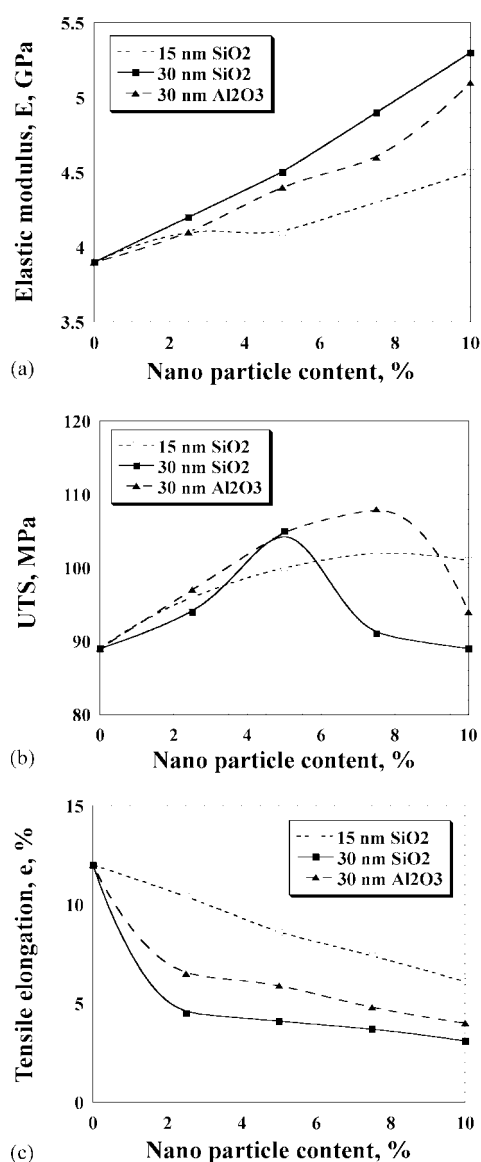


Fig. 2. Variations of the (a) Young's modulus E , (b) ultimate tensile stress (UTS), and (c) tensile failure elongation e of the nanocomposites as a function of the particle content in wt.%.

PEEK was estimated using a Perkin-Elmer thermogravimetry analyzer (TGA-7), running from 25 to 700 °C at a heating rate of 10 °C min⁻¹ under nitrogen atmosphere.

3. Results and discussions

3.1. Microhardness measurements

As shown in Fig. 1, the H_v microhardness readings increased all the way from 21.7 of the pure PEEK polymer to 32.5 in the 10 wt.% 15 nm SiO₂ filled composites, implying a maximum increment percentage of 50%. It has been shown that a composite with a higher hardness value will be accompanied with a lower wear rate and friction coefficient [10–12]. Note that the hardness increment in the SiO₂ filled composites is consistently higher than that in the Al₂O₃ filled ones. However, the intrinsic hardness of the SiO₂ (Mohs scale of 7, and H_v scale around 1000) in glass phase is generally considerably lower than that of Al₂O₃ (Mohs scale of 9, and H_v scale around 1500). The lower H_v for the Al₂O₃ filled composite is thought to result partly from the lower Al₂O₃ volume fraction, and partly from the particle shape effect. The spherical Al₂O₃ particles might impose lower resistance against PEEK segment motion under indentation. The same trend will also be seen from the elastic modulus measurement. Meanwhile, in comparison with the same SiO₂ particles but with different

sizes of 15 and 30 nm, the composites with finer nanoparticles show a continuous and linear hardness increment even at the highest SiO₂ content of 10 wt.%. It seems that the finer 15 nm particles could be more uniformly distributed and contributed the continuous hardness improvement, as discussed later on the base of modulus and UTS data.

Since there is no widely accepted addition rule for the nanocomposite hardness (or modulus and strength), it is simply evaluated by the modified rule of mixture for discontinuous reinforcement [14], i.e.:

$$X_c = \eta X_p V_p + X_m V_m, \quad (1)$$

where X can be hardness, modulus, or tensile strength, V the volume fraction, and the subscripts c, p, and m represent the composite, particle, and matrix, respectively. The strengthening efficiency coefficient η would decrease rapidly with decreasing reinforcement aspect ratio [14]. Extending the values for short fibers with aspect ratios of 10–100 to the range for nanoparticles with an aspect ratio of ~ 1 , η is assumed to be ~ 0.1 . With the best estimations for the Vicker microhardness H_v for the PEEK, SiO₂, and Al₂O₃ to be 21.7, 1000, and 1500, the maximum H_v readings would be 25.5 for the 10 wt.% (4.9 vol.%) SiO₂ filled composite and 25.9 for the 10 wt.% (3.3 vol.%) Al₂O₃ filled composites. The experimentally measured H_v data of 28.2–32.5 are slightly higher than such predicted values. The comparisons between the theoretical and experimental microhardness data on various

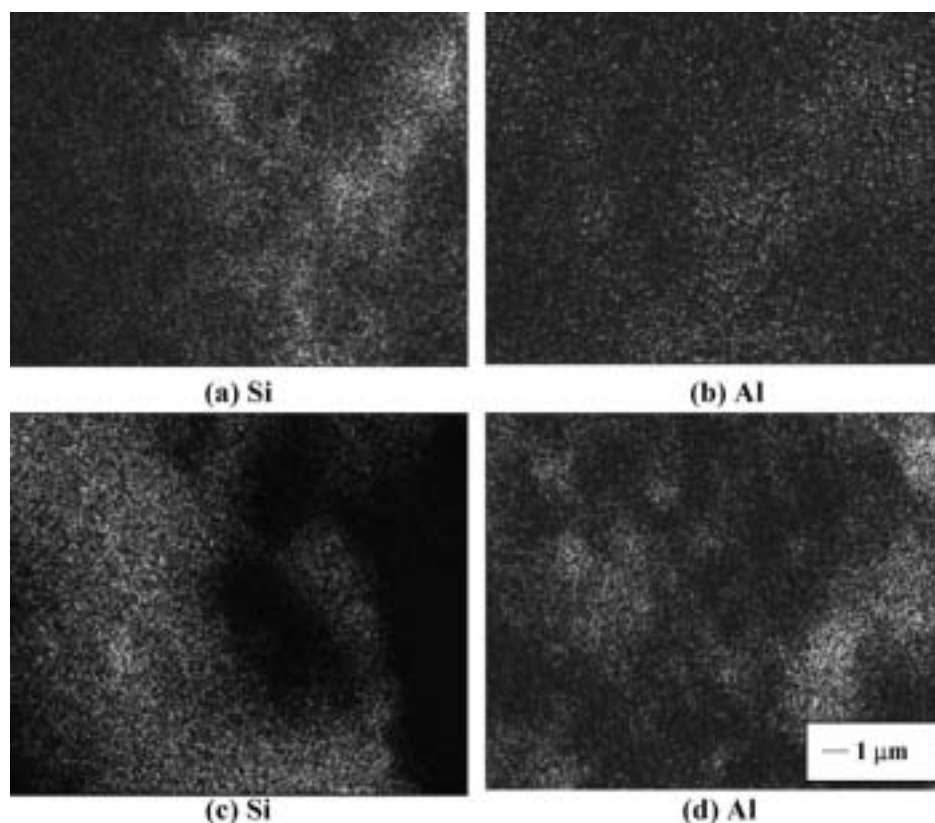


Fig. 3. SEM/EDS elemental mapping (Si or Al) for the composites with: (a) 5 wt.% SiO₂, (b) 5 wt.% Al₂O₃, (c) 7.5 wt.% SiO₂, and (d) 7.5 wt.% Al₂O₃.

nanocomposites, as well as the increment percentage with respect to the unfilled PEEK, are presented in Table 2.

It has been claimed [10] that the wear resistance of PEEK composites filled with larger ZrO_2 nanoparticles measuring 86 nm became worse than that of the unfilled PEEK because of the discontinuous thick transfer film and the weak mutual adhesion. In contrast, the addition of much finer ZrO_2 measuring 10 nm could form a thin, uniform and tenacious transfer film on the counterpart steel surface during the wearing process, leading to a lower frictional coefficient and wear rate of the filled PEEK. It seems that the smaller fillers are more effective in increasing the hardness and lowering the wear rate, as also observed in the current 15 nm SiO_2 composites. For the present PEEK composites containing both 15 and 30 nm nanoparticles and both exhibiting appreciable hardness increment, it is conceivable to expect satisfactory wear improvement in composites filled with 7.5–10 wt.% nanoparticles.

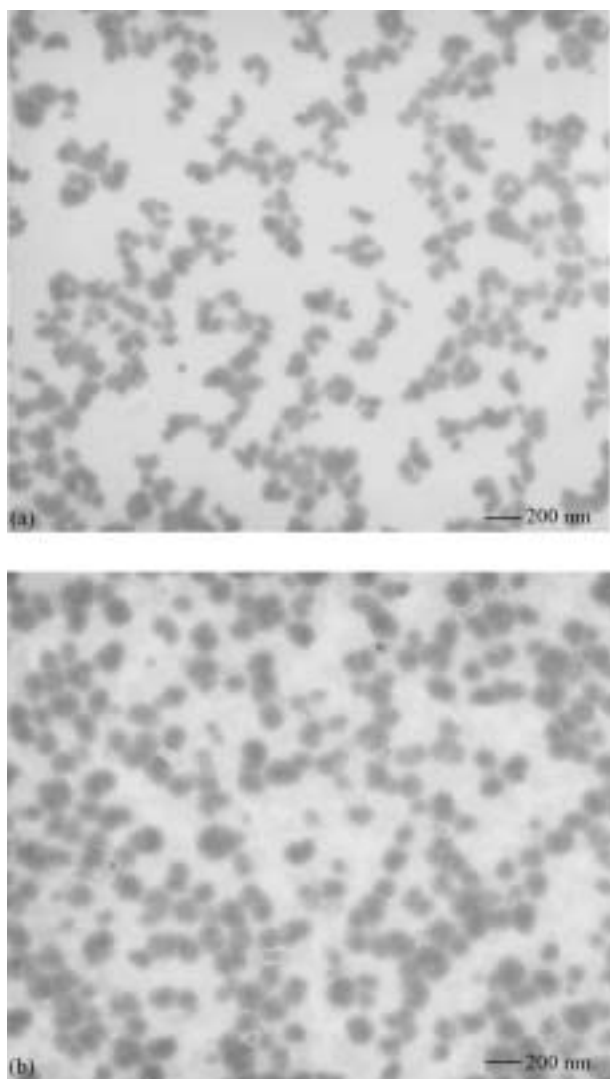


Fig. 4. TEM micrographs showing the distribution of the nanoparticles: (a) 2.5 wt.% SiO_2 and (b) 5 wt.% SiO_2 .

3.2. Tensile properties

The variations of the average data on the Young's modulus (E), ultimate tensile strength (UTS), and failure elongation (e) as a function of nanoparticle content are shown in Fig. 2. The continuous increasing trend of the elastic modulus up to 10 wt.% nanoparticles, as depicted in Fig. 2(a), resembles to that for the hardness. The highest increment occurs in the silica composites with 10 wt.% 30 nm SiO_2 ; raising the PEEK modulus from 3.9 up to 5.3 GPa (or an increment percentage of 36%, Table 2). In comparison, the 30 nm Al_2O_3 nanoparticles provide a slightly lower improvement in the elastic modulus, same as the situation in hardness, presumably due to the lower volume fraction and spherical shape of the Al_2O_3 nanoparticles. As for the SiO_2 nanoparticles with a finer size of 15 nm, the modulus increment was further lower, suggesting that extra fine particles might not be able to elaborate their full strengthening capability in stiffness enhancement. Nevertheless, the more uniform spatial distribution of the finer particles might result in higher strengths as seen later, and higher hardness as mentioned early. The lower modulus should not be owing to a severer nanoparticle clustering since the tensile elongation of this composite is appreciably higher, and the hardness and UTS show continuously increasing trend. It seems that, with the same amount of nanoparticles, finer ones would result in more free volume space between the filled particles, and the polymer chain segments would in turn deform themselves in a more mobile manner, accounting for the lower Young's modulus and higher failure strain.

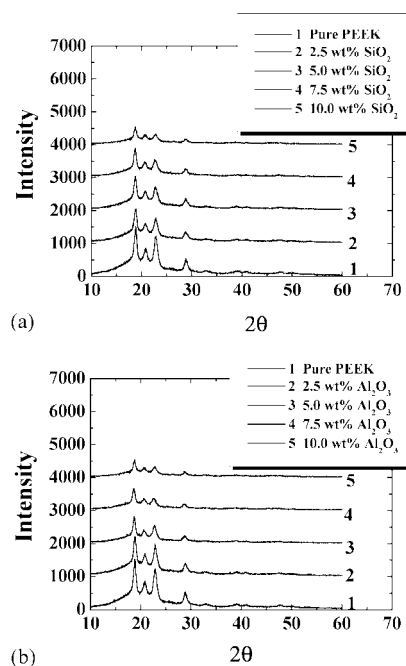


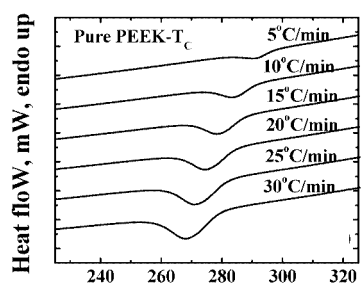
Fig. 5. X-ray diffraction patterns of the PEEK nanocomposites filled with 30 nm (a) SiO_2 and (b) Al_2O_3 particles.

Based on the same argument of the modified rule of mixture, Eq. (1), the maximum predicted composite modulus E_c would be ~ 4.1 for the 10 wt.% (4.9 vol.%) SiO_2 filled composite and ~ 5.0 for the 10 wt.% (3.3 vol.%) Al_2O_3 filled composites, using the modulus data of 3.9, 73, and 393 GPa [15] for PEEK, SiO_2 , and Al_2O_3 , respectively. The experimentally obtained data are again somewhat higher than the predicted ones (Table 2). Theoretically, the modulus for the Al_2O_3 filled composites should be higher, but the experimental data did not reveal such a trend. This might be again due to the spherical shape of Al_2O_3 nanoparticles.

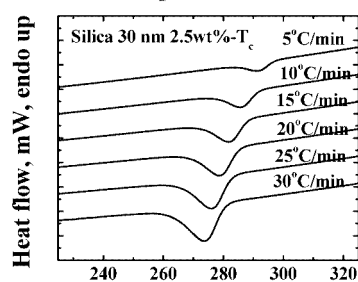
As for the UTS, there shows a maximum peak for all three composites, occurring at a SiO_2 or Al_2O_3 content of 5.0–7.5 wt.%, as depicted in Fig. 2(b) and Table 2. The 15 nm SiO_2 composites behave better, with nil decrement in the 10 wt.% samples, suggesting the best spatial distribution at high filler contents. With a greater amount of nanoparticles, the strength starts to decrease due to local particle clustering and pre-matured failure. Even the Young's modulus and hardness are still increasing at 10 wt.%, the UTS reveals the reversed trend. The highest UTS improvement occurs in the

composites with 7.5 wt.% 30 nm Al_2O_3 to 108 MPa, or an increment percentage of 21% (Table 2). The predicted strength values in Table 2, based on Eq. (1), are ~ 92 for the 10 wt.% (4.9 vol.%) SiO_2 filled composite and ~ 93 for the 10 wt.% (3.3 vol.%) Al_2O_3 filled composites, using the strength data of 89, 1500, and 2000 MPa [15] for PEEK, SiO_2 , and Al_2O_3 .

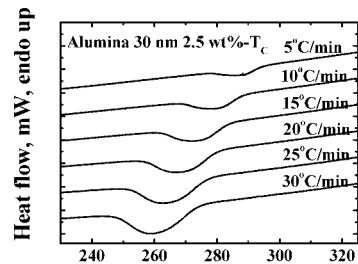
Nevertheless, the tensile failure elongation continuously drops from the 12% of the unreinforced PEEK to 4–6% in the 10 wt.% nanocomposite, as depicted in Fig. 2(c). Composites with the 15 nm nanoparticles consistently exhibit higher tensile elongations than the 30 nm counterparts, suggesting a lower degree of particle clustering and particularly a higher flexibility of PEEK matrix deformation, as discussed above. Note that in Fig. 2(c) the elongation data on the 30 nm Al_2O_3 filled composites are all higher than those on the 30 nm SiO_2 counterparts. This might be due to the spherical shape of the Al_2O_3 nanoparticles, which would usually result in less hindrance when contacting with the polymer segments and more uniform spatial distribution, as well as a lower stress concentration at the particle/matrix interface. All these effects would help to improve the toughness.



(a)

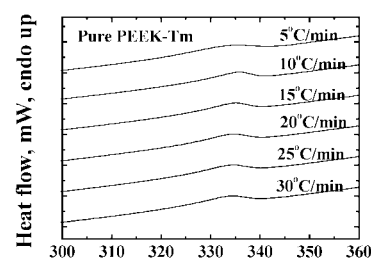


(b)

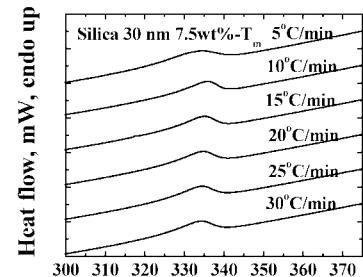


(c)

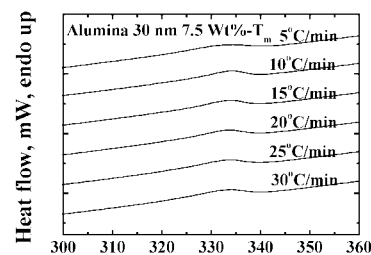
Fig. 6. DSC thermalgrams of the nanocomposites during non-isothermal crystallization at different cooling rates: (a) pure PEEK; (b) 2.5 wt.% 30 nm silica/PEEK; (c) 2.5 wt.% 30 nm alumina/PEEK.



(a)



(b)



(c)

Fig. 7. DSC thermalgrams of the nanocomposites upon heating showing the melting peak: (a) pure PEEK; (b) 7.5 wt.% 30 nm silica/PEEK; (c) 7.5 wt.% 30 nm alumina/PEEK.

3.3. SEM observations

It is well known that the nanoparticles would agglomerate together in the polymer matrix, and in turn decrease the reinforcing effects. The nanoparticles are difficult to be well resolved by the secondary or back scattering electron images under SEM, since the contrast is generally weak. With the help of EDS, it is possible to roughly estimate the dispersion condition of the nanoparticles. Fig. 3 shows the Si or Al EDS mappings for the 5 and 7.5 wt.% 30 nm nanocomposites. It is seen that the dispersion condition of silica and alumina nanoparticles in the PEEK matrix are reasonably uniform in the 2.5 and 5 wt.% composites. Nevertheless, the agglomeration degree increases with increasing nanoparticle content, particularly for the 10 wt.% ones. This is postulated to be caused by the greater viscosity of the PEEK/nanoparticles mixture at higher nanoparticle contents during the hot press processing.

By closer examinations, the local clustering effect is less severe in the Al₂O₃ composites. This is postulated to be caused by the spherical shape of Al₂O₃ making the particle flow and dispersion in the PEEK matrix to proceed more smoothly. It is also consistent with the observation that the 30 nm SiO₂ composites start to decline in UTS at

7.5 wt.%, while the Al₂O₃ composites still show strengthening at 7.5 wt.% (Fig. 2(b) and Table 2). Meanwhile, the agglomeration is also less pronounced in the 15 nm composites. It follows that the UTS of the 15 nm SiO₂ composites remain its high level even at 10 wt.%. It is conceivable that, with further improvement of nanoparticle clustering via particle surface modification, though more expensive, the mechanical properties can be further upgraded. However, for wear rate reduction, the current simple processing route appears to be adequate.

3.4. TEM observations

Systematic examinations on the dispersion of the nano SiO₂ or Al₂O₃ particles in various composite specimens have been conducted. Fig. 4 presents some typical examples of the TEM micrographs taken from the 30 nm 2.5 and 5 wt.% SiO₂ composites. Although there are occasional clustering occurrences for two to five nanoparticles to cluster or align together, the majority of the nanoparticles were seen to disperse semi-homogeneously in the PEEK matrix.

The relatively satisfactory dispersion of the current SiO₂ or Al₂O₃ particles, independent of 15 or 30 nm in size, may be due to the sound mixture through ultrasonic vibration in

Table 3
DSC data on the 15 nm silica filled PEEK composites, obtained from the cooling DSC runs

Sample	Cooling rate (°C s ⁻¹)	T _m (°C)	T _{ci} (°C)	T _{ep} (°C)	T _{cf} (°C)	H _c (J g ⁻¹)	X _c (%)
Pure PEEK	5	337	302	296	285	-40.4	31.1
	10	339	297	289	278	-33.1	25.5
	15	338	293	284	273	-30.0	23.1
	20	338	290	280	269	-29.1	22.4
	25	338	288	277	265	-27.7	21.3
	30	337	286	274	262	-26.7	20.5
SiO ₂ , 2.5 wt.%	5	333	299	292	283	-52.1	41.1
	10	335	305	280	267	-42.7	33.6
	15	335	301	272	260	-38.0	29.9
	20	335	288	266	254	-35.2	27.8
	25	334	283	262	249	-34.3	27.1
	30	334	278	268	245	-33.2	26.2
SiO ₂ , 5 wt.%	5	335	299	291	271	-63.5	51.4
	10	338	294	284	268	-47.2	38.2
	15	337	290	280	262	-42.0	34.0
	20	337	287	275	259	-38.1	30.8
	25	336	284	273	256	-34.0	27.6
	30	336	281	269	253	-32.7	26.5
SiO ₂ , 7.5 wt.%	5	335	298	291	274	-43.3	36.0
	10	338	295	284	271	-38.0	31.6
	15	338	292	279	265	-37.0	30.8
	20	338	288	276	261	-36.1	30.1
	25	336	286	273	258	-33.5	27.9
	30	336	283	270	255	-32.6	27.1
SiO ₂ , 10 wt.%	5	337	296	290	272	-31.7	27.0
	10	338	292	283	272	-30.4	26.0
	15	338	288	278	266	-29.9	25.6
	20	337	285	274	261	-28.1	24.0
	25	337	283	272	258	-27.4	23.4
	30	337	281	269	254	-27.0	23.0

T_{ci}, T_{ep}, and T_{cf} are referred to the initiation, peak, and finishing temperatures for PEEK crystallization, respectively.

alcohol medium, as well as the high load applied during the forming. The latter would force the highly viscous PEEK polymer to flow during the intensive flow the nanoparticles would be forced to disperse separately.

3.5. X-ray diffraction analysis

For better understanding of the possible chemical interactions between the nanoparticles and the PEEK matrix, X-ray diffraction was applied to determine the effect of filler content on the d -spacing of the crystalline PEEK. With the addition of silica or alumina nanoparticles from 2.5 to 10 wt.%, there is no extra peak created or disappeared as compared with those of the pure PEEK, as shown in Fig. 5. The SiO₂ or Al₂O₃ diffractions are too low to be resolved in Fig. 5. It appears that there is no apparent interaction that would result in appreciable new interfacial phases. The weaker diffraction intensity in composites with a high amount of nanoparticles was mainly due to the smaller PEEK crystallites, coupled with the lower PEEK weight fraction. For the composites with a high fraction of nanoparticles (e.g. 10%), a lower degree of crystallization might sometimes occur, since the PEEK matrix filled with abundant SiO₂ or Al₂O₃ would decrease the mobility of the

polymer chain segments during the period of crystallization [16–18].

3.6. DSC analysis on non-isothermal crystallization

The non-isothermal crystallization behaviors of the nanocomposites were studied by DSC, with the samples cooled from 410 to 50 °C at constant cooling rates of 5, 10, 15, 20, 25, and 30 °C min⁻¹. As shown in Fig. 6, the crystallization initiation, peak, and finishing temperatures, T_{ci} , T_{cp} , and T_{cf} , shifts to lower temperatures, for both the PEEK and nanoparticle-filled PEEK, as the cooling rate increases. The faster is the cooling rate, the greater supercooling is required to initiate the crystallization of the PEEK chain segments since the motion speed of the PEEK chain segments could not catch up the cooling rate [19]. Also, there is no significant change in the melting points, T_m , of both the filled and unfilled specimens in the DSC diagram, as shown in Fig. 7. The melting temperatures are consistently scattered within $337 \pm 3^\circ$, in the typical range of 330–385 °C for PEEK resin. As for the addition of nanoparticles on the crystallization of PEEK, there are several factors involved; some of them are counteracting each other making the net effect obscure sometimes. For example, in terms of heterogeneous nucleation of

Table 4
DSC data on the 30 nm silica filled PEEK composites, obtained from the cooling DSC runs

Sample	Cooling rate (°C s ⁻¹)	T_m (°C)	T_{ci} (°C)	T_{cp} (°C)	T_{cf} (°C)	H_c (J g ⁻¹)	X_c (%)
Pure PEEK	5	337	302	296	285	-40.4	31.1
	10	339	297	289	278	-33.1	25.5
	15	338	293	284	273	-30.0	23.1
	20	338	290	280	269	-29.1	22.4
	25	338	288	277	265	-27.7	21.3
	30	337	286	274	262	-26.7	20.5
SiO ₂ , 2.5 wt.%	5	336	303	296	288	-41.3	32.6
	10	339	297	291	281	-38.0	29.9
	15	338	293	287	277	-36.5	28.8
	20	337	290	284	273	-35.6	28.1
	25	337	288	281	270	-35.1	27.7
	30	337	286	279	267	-34.7	27.3
SiO ₂ , 5 wt.%	5	337	303	297	290	-43.9	35.6
	10	340	299	292	282	-40.7	33.0
	15	340	296	289	277	-38.9	31.5
	20	339	293	286	273	-37.7	30.5
	25	339	291	283	270	-37.1	30.0
	30	339	289	281	267	-36.2	29.3
SiO ₂ , 7.5 wt.%	5	338	300	295	288	-39.9	33.1
	10	339	300	289	280	-39.2	32.5
	15	339	297	284	275	-38.5	32.0
	20	338	294	281	271	-38.0	31.7
	25	338	292	278	267	-36.8	30.6
	30	338	291	276	265	-35.8	29.7
SiO ₂ , 10 wt.%	5	338	300	293	286	-32.1	27.3
	10	340	296	287	278	-29.0	24.8
	15	339	292	282	273	-28.7	24.6
	20	339	289	279	269	-28.0	23.9
	25	339	287	276	266	-27.7	23.7
	30	338	285	274	263	-27.0	23.0

T_{ci} , T_{cp} , and T_{cf} are referred to the initiation, peak, and finishing temperatures for PEEK crystallization, respectively.

Table 5
DSC data on the 30 nm alumina filled PEEK composites, obtained from the cooling DSC runs

Sample	Cooling rate ($^{\circ}\text{C s}^{-1}$)	T_m ($^{\circ}\text{C}$)	T_{ci} ($^{\circ}\text{C}$)	T_{cp} ($^{\circ}\text{C}$)	T_{cf} ($^{\circ}\text{C}$)	H_c (J g^{-1})	X_c
Pure PEEK	5	337	302	296	285	-40.4	31.1
	10	339	297	289	278	-33.1	25.5
	15	338	293	284	273	-30.0	23.1
	20	338	290	280	269	-29.1	22.4
	25	338	288	277	265	-27.7	21.3
	30	337	286	274	262	-26.7	20.1
Al_2O_3 , 2.5 wt.%	5	337	298	293	280	-58.8	46.4
	10	339	294	284	271	-49.8	39.2
	15	339	289	279	265	-45.8	36.1
	20	338	286	274	260	-42.9	33.8
	25	338	283	269	256	-40.8	32.1
	30	338	280	265	252	-39.2	31.0
Al_2O_3 , 5 wt.%	5	337	295	285	278	-49.1	39.8
	10	339	288	277	269	-43.1	34.9
	15	338	283	271	262	-39.9	32.3
	20	338	279	267	257	-37.9	30.7
	25	337	276	263	252	-36.6	29.7
	30	337	273	260	248	-35.1	28.4
Al_2O_3 , 7.5 wt.%	5	335	295	285	277	-44.3	36.9
	10	338	287	277	268	-38.7	32.2
	15	337	282	271	261	-35.1	29.2
	20	337	279	267	256	-33.5	27.9
	25	337	276	264	251	-30.5	25.4
	30	336	274	260	247	-28.4	23.6
Al_2O_3 , 10 wt.%	5	335	294	285	277	-45.3	38.7
	10	337	287	277	267	-39.1	33.4
	15	336	282	272	261	-36.0	30.8
	20	336	279	268	256	-34.2	29.2
	25	335	277	265	251	-32.8	28.0
	30	335	274	262	248	-30.9	26.4

T_{ci} , T_{cp} , and T_{cf} are referred to the initiation, peak, and finishing temperatures for PEEK crystallization, respectively.

PEEK on the nanoparticle interfaces, the crystallization initiation and peak temperature might increase. However, the obstacle effect from the nanoparticles on the PEEK mobility and crystallization would lower the crystallization temperatures. Tables 3–5 summarize the data on T_m , T_{ci} , T_{cp} , T_{cf} , and the crystallization enthalpy, H_c , for the pure PEEK and nanocomposites.

From the DSC curves, the absolute crystallinity fraction X_c at different cooling rates can be estimated by relating to the heat of fusion of an infinitely thick PEEK crystal, ΔH_f° , as [13]:

$$X_c = \frac{\Delta H_c}{\Delta H_f^{\circ} W_{\text{polymer}}} \times 100, \quad (2)$$

where ΔH_f° is $\sim 130 \text{ J g}^{-1}$ [20] and W_{polymer} the weight fraction of polymer matrix. As shown in Tables 3–5, it is obvious that a slower cooling rate would result in a slightly higher crystallinity value, as a result of more sufficient time for crystallization. Furthermore, the inclusion of nanoparticles, independent of silica or alumina, would increase the crystallinity fraction. X_c was seen to increase from 20 to 30% for the pure PEEK to 25–50% for the composites, particularly for lower nanoparticle contents such as 2.5 and 5.0 wt.%. The heteroge-

neous nucleation on the existing nano-sized silica or alumina should be responsible for the increases of the crystallinity in the composites [19]. When the nanoparticle content is continuously increased to 7.5 or 10 wt.%, the crystallinity fraction increment becomes minor, accounting for the lower mobility of the PEEK chain segments at high nanoparticle contents. For the composites with 10 wt.% 15 or 30 nm SiO_2 , the irregular shape of the SiO_2 particles might have clustered in certain positions. This would lower the available heterogeneous nucleation sites for PEEK crystallization at the interfaces, and sometimes even lower crystallinity fraction X_c values.

In comparing the X_c values for composites filled with the same amount of SiO_2 nanoparticles but with different sizes of 15 and 30 nm, the finer particles would lead to a higher crystallinity fraction. This might be due to the lower degree of obstruction from the finer particles for the extension of PEEK crystalline segments. In comparing X_c for composites filled with different particles of SiO_2 or Al_2O_3 , the Al_2O_3 nanoparticles seem to induce higher X_c values. It is postulated to be caused again by the spherical shape and the more uniform distribution of Al_2O_3 , thus providing more nucleation sizes. By closer examinations of the DSC curves in Fig. 5, the shape and the extending temperature range of the exothermic peaks in the SiO_2 and Al_2O_3 filled composites are slightly differ-

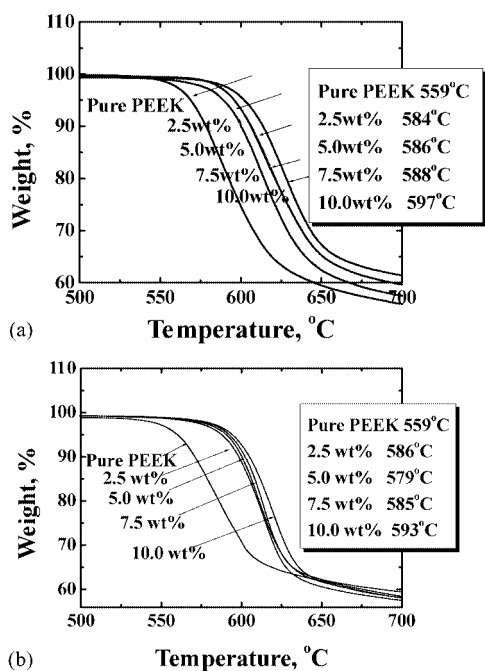


Fig. 8. The TGA diagrams of the PEEK nanocomposites filled with 30 nm (a) SiO₂ and (b) Al₂O₃ particles.

ent, suggesting that the PEEK crystallization details might differ slightly. Systematic studies on the PEEK crystallization kinetic mechanisms in various nanocomposites will be a subject of further studies.

The DSC results, coupled with the XRD patterns, suggest that there has been minimum chemical interaction between the PEEK polymer and ceramic nanoparticles occurred at the forming temperature of 400 °C. But the crystallization temperature and crystallinity fraction X_c of the PEEK matrix would be affected by the amount of nanoparticles, with the melting temperature T_m of PEEK matrix unchanged.

3.7. TGA measurements

It has been proposed that a polymer resin reinforced with nano-sized inorganic particulates would improve its thermal stability, including the resistances of thermal degradation and flammability. Therefore, it is desired to estimate the resistance of thermal degradation of the current PEEK composites. Fig. 8 shows the TGA results. It can be seen that with increasing nanoparticle content, the degradation temperature T_D of the PEEK polymer continuously increases. With a silica content of 10 wt.%, T_D can be raised by nearly 40 °C. It is considered to be an appreciable improvement of the thermal stability.

4. Conclusions

1. Irrespective of silica or alumina particles filled, the PEEK based nanocomposites can improve their hardness, elas-

tic modulus, and tensile strength by 20–50%, with the sacrifice of tensile elongation. The maximum increment percentages with respect to the unfilled PEEK are 50, 36, and 21% for hardness, elastic modulus, and UTS, respectively.

2. The optimum strengthening improvement occurs in composites filled with 5.0–7.5 wt.% (or 2–4 vol.%) nanoparticles. With a greater amount to 10 wt.%, the clustering problem would start to lower the tensile strength, but still continuously upgrade the hardness and elastic modulus. In terms of wear applications, a higher nanoparticle content is desired.
3. Theoretically, the harder nanoparticles with a spherical shape would lead to more uniform spatial dispersion and more efficient strengthening. Extra fine nanoparticles measuring around 15 nm seem to elaborate a lower strengthening efficiency in stiffness than the 30 nm ones, but providing a more uniform spatial distribution and a lower loss of the ductility.
4. The modified rule of mixture originally for short-fiber reinforced composites can provide a rough strengthening trend for the nanocomposites, but the predicted values are typically lower than the measured data.
5. There is no apparent interaction occurred between the nanoparticles and the PEEK matrix during the hot pressing at 400 °C, based on the XRD and DSC results.
6. The inclusion of silica or alumina nanoparticles to limited amounts will increase the degree of crystallinity of the resulting nanocomposites, as compared with the pure PEEK polymer.
7. The inclusion of the inorganic filler into PEEK matrix can improve the thermal stability of the resulting nanocomposites by 40 °C.

Acknowledgements

The authors would like to gratefully acknowledge the sponsorship from National Science Council of Taiwan, ROC, under the project no. NSC 92-2216-E-110-017.

References

- [1] R.N. Rethon, Adv. Polym. Sci. 139 (1999) 67.
- [2] R.N. Rethon, Adhesion 64 (1997) 87.
- [3] W.H. Bonner, U.S. Patent 3,065,205 (1962).
- [4] T.E. Attwood, P.C. Dawson, J.L. Freeman, L.R.J. Hoy, J.B. Rose, P.A. Staniland, Polymer 22 (1981) 1096.
- [5] S.L. Gao, J.K. Kim, Composites A 31 (2000) 517.
- [6] M.C. Kuo, J.C. Huang, M. Chen, M.H. Jen, Mater. Trans. 44 (2003) 1613.
- [7] M. Zhang, J. Xu, Z. Zhang, H. Zeng, X. Xiong, Polymer 37 (1996) 5151.
- [8] T.Q. Li, M.Q. Zhang, K. Zeng, H.M. Zeng, Compos. Sci. Technol. 60 (2000) 465.
- [9] M.C. Wijers, M. Jin, M. Wessling, H. Strathmann, J. Membr. Sci. 147 (1998) 117.

- [10] Q.-H. Wang, J. Xu, W. Shen, W. Liu, *Wear* 196 (1996) 82.
- [11] Q.-H. Wang, Q. Xue, H. Liu, W. Shen, J. Xu, *Wear* 198 (1996) 216.
- [12] Q.-H. Wang, J. Xu, W. Shen, Q. Xue, *Wear* 209 (1997) 316.
- [13] J. Sandlera, P. Werner, M.S.P. Shaffera, V. Demchukc, V. Altstadt, A.H. Windlea, *Composites A* 33 (2002) 1033.
- [14] D. Hull, *An Introduction to Composite Materials*, Cambridge University Press, Cambridge, UK, 1981, pp. 81–101.
- [15] W.D. Callister Jr, *Materials Science and Engineering: An Introduction*, 6th ed., Wiley, New York, USA, 2003.
- [16] G. Tsagaropoulos, A. Eisenberg, *Macromolecules* 28 (1995) 396.
- [17] G. Tsagaropoulos, A. Eisenberg, *Macromolecules* 28 (1995) 6067.
- [18] V. Arrighia, I.J. McEwena, H. Qiana, M.B. Serrano Prietob, *Polymer* 44 (2003) 6259.
- [19] S.H. Kim, S.H. Ahn, T. Hirai, *Polymer* 44 (2003) 5625.
- [20] C.L. Wei, M. Chen, F.E. Yu, *Polymer* 44 (2003) 8185.